Towards A More Rigorous Boresight Calibration[1]

J. Skaloud, P. Schaer

Swiss Federal Institute of Technology Lausanne (EPFL)

Keywords: Boresight, Calibration, Exterior orientation, Direct sensor orientation, Methods, Adjustment

Abstract

This work focuses on the stochastic properties of boresight determination between a strapdown IMU and a frame-based imaging sensor. The core of the stochastic model is a rigorous error propagation of the estimated input accuracies and their correlations. This subsequently yields more realistic estimates of boresight accuracy for every image event. The nature of INS/GPS integration makes the residual orientation errors be strongly correlated within a flight line while little horizontal acceleration is sensed. This information is partially carried within the Kalman filter used for the data integration; however, it is rarely made accessible to the user. As an alternative, we propose estimating the temporal correlations by means of a simplified function that is derived from the flying profile and the inertial system used. Numerical examples are demonstrated for the case of high-resolution digital imagery, where the application of the proposed method allows reaching sub-pixel accuracy in direct georeferencing (e.g. forward intersection without an adjustment).

1. Introduction

One of the common approaches in determining the boresight angles consists in comparing the INS(/GPS) attitude with that obtained by aero-triangulation (AT). This is usually accomplished either within the so-called '2-step' procedure, where the boresight estimation is obtained for every image separately and then averaged [1], [2] (possibly with weights), or by introducing IMU orientation as additional observations in the bundle adjustment and estimating the boresight as one of its parameters [3], [4], [5], [6], [7], [8]. The latter approach is sometimes referred to as "1-step" procedure and has become quite popular despite its tendency to provide too optimistic estimates, as will be discussed further. One can also envisage an approach where the boresight gets estimated as a state-vector parameter of an inertial navigator using AT-data as additional updates of the Kalman Filter. Finally, considering global adjustment of all data sources as an additional option, we summarize these concepts in Table 1.

Approach	Adjustment Space	Additional Observations	Considering time correlations in IMU data?	Remark
"No step"	Global	IMU, GPS, AT, (GCP)	Yes	Not developed, optimal but cumbersome.
" 1 step"	AT	IMU/GPS, (GCP)	No (→Yes possible)	Too optimistic accuracy estimate. Biased mean?
" Reversed 1 step"	IMU	/GPS, /Attitude_AT	Yes	Not developed, may lead to KF divergence.
"2 steps"	Additional /Independent	IMU/GPS, AT (Attitude only)	Yes	Developer independent, presented method.

Table 1. Conceptual approaches to boresight determination with respect to IMU/GPS attitude correlation.

The degree of rigor sustained by the above mentioned approaches often reflects the available tools and the background of the personnel performing this task rather than the theoretical outcome that would perhaps equalize all approaches under flawless stochastic assumptions. Leaving these perhaps decisive aspects aside, there are two additional factors playing a vital role in the quality of boresight estimate: first, the method's ability in detecting blunders, systematic errors and providing overall robust quality control [9], second, accounting for significant correlations (spatial or temporal) that appear between the measurements. As very strong temporal correlations are inherently present in all IMU/GPS systems, failing to acknowledge this fact leads to biased mean-values and over-optimistic estimates of boresight accuracy as will be demonstrated later on. Currently implemented '1-step' approaches suffer from such negligence, mainly due to the following reasons:

[1] ISPRS International Workshop on Theory, Technology and Realities of Inertial / GPS Sensor Orientation, Commission 1, WG I/5, Castelldefels, Spain, 22.-23. September 2003.

- The IMU/GPS systems output orientation accuracy without indicating its temporal correlation
- The AT software is not adapted to handle complicated structure of IMU/GPS temporal correlation

This contribution aims to remove such setback by proposing a general "2-step" procedure that accounts for the temporal correlation (IMU/GPS) as well as space correlations (AT) in the orientation data. First, we present the functional and the stochastic model of this approach. Then we examine the alternative ways of determining the proper weights (correlation factors) when the user has a restricted or no access to KF variance-covariance matrix. Finally, we present numerical examples and discuss the practical considerations.

2. Functional Model

Considering the law of random error propagation the "2-step" approach essentially corresponds to "1-step" method that is executed in two phases and the outcome of which is identical. As we will try to investigate the effect of correlation between the IMU/GPS orientation on boresight it will be, however, much simpler to work initially only with the orientation data. The advantage of this approach will also be a relative independence from the existing implementations in AT or IMU/GPS data adjustment packages. The functional model thus remains simple as it consists of a comparison between AT (R^c_{enu}) and IMU/GPS 'corrected' (R^b_{enu}) rotational matrices for n image events ('*ENU*' = east-north-up):

$$R^c_{b_i} = R^c_{enu_i}\left(R^b_{enu_i}\right)^T, i = 1,2,\ldots,n \tag{1}$$

The need for IMU/GPS attitude correction stems from the fact that the inertial navigator usually provides the body (b) attitude with respect to the local-level axes, whose orientation in space corresponds to its actual geographical position and therefore varies with the movement of the sensor. Considering a conformal tangential projection used by AT with '*ENU*' coordinate axes orientation of a fixed origin and the inertial navigator's attitude with respect to the local-level '*NED*' (north-east-down) axes, the alignment to a common orientation reference takes the form:

$$R^b_{enu_i} = R^b_{ned_i} R^{ned_i}_{ned_0} T^{ned}_{enu} \tag{2}$$

It should be noted that the ned_0 to ned_i rotation is fairly small (<3°) over medium-size mapping areas and therefore can be neglected when studying the covariance propagation later on. Similarly, T is a reflection matrix that swaps roll with pitch and changes the sign of the heading. As the accuracy of roll and pitch tends to be similar, we may also neglect this transformation for the sake of simplicity, despite the fact that this matrix will not be needed when using an inertial navigation with '*ENU*' implementation. Again, such simplifications are only possible when caring about boresight accuracy, not its value!

A direct comparison of Euler angles is possible only for small rotation, which means that the boresight should not exceed few degrees per axis when using such approach. This is, however, the case in practical applications as the larger differences in IMU-camera orientation due to installation (often ±π/2) are known and thus can be accounted for prior to the processing of the inertial data. Hence, the boresight matrix in equation (1) can take upon a skew-symmetric form:

$$R^c_{enu_i} = \begin{bmatrix} c_{11} & c_{12} & c_{13} \\ c_{21} & c_{22} & c_{23} \\ c_{31} & c_{32} & c_{33} \end{bmatrix} = \begin{bmatrix} 1 & e_c & -e_b \\ -e_c & 1 & e_a \\ e_b & -e_a & 1 \end{bmatrix} \begin{bmatrix} r_{11} & r_{12} & r_{13} \\ r_{21} & r_{22} & r_{23} \\ r_{31} & r_{32} & r_{33} \end{bmatrix} = R^c_{b_i} R^b_{enu_i} \tag{3}$$

As suggested in [2] this relation can be used to form nine equations that link the unknown boresight vector x = [2] to the observations l that are formed by the differences between the corresponding coefficients in the rotation matrices. With residuals v we obtain for each $R^c_{b_i}$

$$l + v = A_i x$$

$$l_{j+3(k-1)} = c_{j,k} - r_{j,k} \qquad j,k = 1,2,3 \tag{4}$$

$$A_i^t = \begin{bmatrix} 0 & 0 & 0 & r_{31} & r_{32} & r_{33} & -r_{21} & -r_{22} & -r_{23} \\ -r_{31} & -r_{32} & -r_{33} & 0 & 0 & 0 & r_{11} & r_{12} & r_{13} \\ r_{21} & r_{22} & r_{23} & -r_{11} & -r_{12} & -r_{13} & 0 & 0 & 0 \end{bmatrix}$$

Using n images thus produces $9n$ 'observations' that can be adjusted by a least-square principle when forming three normal equations N and estimating the x as:

$$N = {}_{9n}A_3^t \, {}_{9n}P_{9n} \, {}_{9n}A_3$$
$$x = N^{-1}A^t Pl \tag{5}$$

It should be noted, however, that the 9 elements of full-rotational matrix are correlated among themselves and so it is then our 9-element observation vector. The $R^b_{enu_i}$ matrices are further correlated among themselves as stems from the nature of inertial navigation. Hence, considering the P matrix as an identity or a matrix with values only on the main diagonal will certainly violate the assumptions needed to obtain an unbiased estimate in the least-square sense.

An alternative approach is to work directly with the skew-symetric matrices obtained by relation (1) the triplet of which contains only 'independent' elements. These can be extracted from each observed skew-symetric matrix and the mean boresight angles estimated from a weighted average (p):

$$\bar{e}_a = \sum_{i=1}^{n} e_{a_i} p_{a_i}, \bar{e}_b = \sum_{i=1}^{n} e_{b_i} p_{b_i}, \bar{e}_c = \sum_{i=1}^{n} e_{c_i} p_{c_i} , \tag{6}$$

As in the previous case, setting the proper weights p will play a decisive role on the estimate as varying accuracies and correlations need to be accounted for. We shall investigate this when examining closely the error propagation in the next section.

3. Stochastic Model with Temporal Correlations

According to (1) each element of the boresight alignment matrix is a function of camera orientation (ω, φ, κ), and IMU/GPS attitude (r, p, y), i.e. we can write:

$$R^c_{b_i} = f(\omega, \varphi, \kappa, r, p, y) = \begin{bmatrix} b_{11} & b_{12} & b_{13} \\ b_{21} & b_{22} & b_{23} \\ b_{31} & b_{32} & b_{33} \end{bmatrix} \tag{7}$$

3.1. Error propagation (Q_{xx})

To study the complete correlation pattern in the boresight estimate we apply the law of random error propagation and transform the initial variance-covariance information (Q_{ll}) as

$$Q_{xx} = F^t Q_{ll} F \tag{8}$$

Considering the dependences (7), matrix F^t [9x6] will contain the partial derivates of the individual rotational elements with respect to each angle as:

$$F^t_i = \begin{bmatrix} \frac{\partial b_{11}}{\partial \varphi} & \frac{\partial b_{11}}{\partial \omega} & \frac{\partial b_{11}}{\partial \kappa} & \frac{\partial b_{11}}{\partial r} & \frac{\partial b_{11}}{\partial p} & \frac{\partial b_{11}}{\partial y} \\ \vdots & \vdots & \vdots & \vdots & \vdots & \vdots \\ \frac{\partial b_{33}}{\partial \varphi} & \frac{\partial b_{33}}{\partial \omega} & \frac{\partial b_{33}}{\partial \kappa} & \frac{\partial b_{33}}{\partial r} & \frac{\partial b_{33}}{\partial p} & \frac{\partial b_{33}}{\partial y} \end{bmatrix}_i \tag{9}$$

The formation of the partial derivatives will depend on the rotational sequences that parameterize the individual orientation matrices and therefore the analytical formulas may vary from case to case. However, there is no practical need to carry out such cumbersome calculations, as a numerical derivation will do just as well. To compute the attitude error propagation for n images in one step, a 'global' F^t matrix [$9n$ x $6n$] is formed:

$$F^t = \begin{bmatrix} F^t_1 & \cdots & 0 \\ \vdots & \ddots & \vdots \\ 0 & \cdots & F^t_n \end{bmatrix} \tag{10}$$

3.2. Construction of the general stochastic model (Q_{ll})

Equation (8) propagates the stochastic information contained in the original variance-covariance matrix Q_{ll}. The information needed for its construction is the following:

σ_φ, σ_ω, σ_κ: AT-estimated accuracy of exterior orientation (attitude only),

$\rho_{\varphi\kappa}, \rho_{\kappa\omega}, \rho_{\varphi\omega}$: optional correlations between (ω, φ, κ) from AT (when available),
σ_r, σ_p, σ_y: IMU/GPS estimated attitude accuracy
σ_{rp}, σ_{py}, σ_{yr}: optional correlations between (r, p, y) from IMU/GPS (when available),
$\rho_{r_t r_{t+\Delta t}}, \rho_{p_t p_{t+\Delta t}}, \rho_{y_t y_{t+\Delta t}}$: Temporal correlation between IMU angles from KF or empirically estimated.

The resulting 'global' Q_{ll} matrix for n-images will have a size of [$6n$ x $6n$]. Considering a scenario when the navigation software characterizes its estimated attitude accuracy only by the square-root of the main diagonal[2], the variance-covariance matrix takes a form:

Image 1 *Image 2* *Image n*

$$Q_{ll} = \left[\begin{array}{cccccc|cccccc|c|cccccc}
\sigma_{\varphi_1}^2 & \sigma_{\varphi_1\omega_1} & \sigma_{\varphi_1\kappa_1} & 0 & \cdot & 0 & 0 & \cdot & \cdot & \cdot & \cdot & 0 & & 0 & \cdot & \cdot & \cdot & \cdot & 0 \\
\sigma_{\varphi_1\omega_1} & \sigma_{\omega_1}^2 & \sigma_{\omega_1\kappa_1} & \cdot & \cdot & \cdot & \cdot & \cdot & \cdot & \cdot & \cdot & \cdot & & \cdot & \cdot & \cdot & \cdot & \cdot & \cdot \\
\sigma_{\varphi_1\kappa_1} & \sigma_{\omega_1\kappa_1} & \sigma_{\kappa_1}^2 & 0 & \cdot & \cdot & \cdot & \cdot & 0 & \cdot & \cdot & \cdot & \cdots & \cdot & \cdot & 0 & \cdot & \cdot & \cdot \\
0 & \cdot & 0 & \sigma_{r_1}^2 & \cdot & \cdot & \cdot & \cdot & \cdot & \sigma_{r_1r_2} & \cdot & \cdot & & \cdot & \cdot & \cdot & \sigma_{r_1r_n} & \cdot & \cdot \\
\cdot & \cdot & \cdot & \cdot & \sigma_{p_1}^2 & \cdot & \cdot & \cdot & \cdot & \cdot & \sigma_{p_1p_2} & 0 & & \cdot & \cdot & \cdot & \cdot & \sigma_{p_1p_n} & 0 \\
0 & \cdot & \cdot & \cdot & \cdot & \sigma_{y_1}^2 & 0 & \cdot & \cdot & \cdot & 0 & \sigma_{y_1y_2} & & 0 & \cdot & \cdot & \cdot & 0 & \sigma_{y_1y_n} \\
\hline
0 & \cdot & \cdot & \cdot & \cdot & 0 & \sigma_{\varphi_2}^2 & \sigma_{\varphi_2\omega_2} & \sigma_{\varphi_2\kappa_2} & \cdot & \cdot & 0 & & 0 & \cdot & \cdot & \cdot & \cdot & 0 \\
\cdot & \cdot & \cdot & \cdot & \cdot & \cdot & \sigma_{\varphi_2\omega_2} & \sigma_{\omega_2}^2 & \sigma_{\omega_2\kappa_2} & \cdot & \cdot & \cdot & & \cdot & \cdot & \cdot & \cdot & \cdot & \cdot \\
\cdot & \cdot & 0 & \cdot & \cdot & \cdot & \sigma_{\varphi_2\kappa_2} & \sigma_{\omega_2\kappa_2} & \sigma_{\kappa_2}^2 & \cdot & \cdot & \cdot & \cdots & \cdot & \cdot & 0 & \cdot & \cdot & \cdot \\
\cdot & \cdot & \cdot & \sigma_{r_1r_2} & \cdot & \cdot & \cdot & \cdot & \cdot & \sigma_{r_2}^2 & \cdot & \cdot & & \cdot & \cdot & \cdot & \sigma_{r_2r_n} & \cdot & \cdot \\
\cdot & \cdot & \cdot & \cdot & \sigma_{p_1p_2} & 0 & \cdot & \cdot & \cdot & \cdot & \sigma_{p_2}^2 & \cdot & & \cdot & \cdot & \cdot & \cdot & \sigma_{p_2p_n} & 0 \\
0 & \cdot & \cdot & \cdot & 0 & \sigma_{y_1y_2} & 0 & \cdot & \cdot & \cdot & \cdot & \sigma_{y_2}^2 & & 0 & \cdot & \cdot & \cdot & 0 & \sigma_{y_2y_n} \\
\hline
 & & \vdots & & & & & & \vdots & & & & \ddots & & & \vdots & & & \\
\hline
0 & \cdot & \cdot & \cdot & \cdot & 0 & 0 & \cdot & \cdot & \cdot & \cdot & 0 & & \sigma_{\varphi_n}^2 & \sigma_{\varphi_n\omega_n} & \sigma_{\varphi_n\kappa_n} & \cdot & \cdot & 0 \\
\cdot & \cdot & \cdot & \cdot & \cdot & \cdot & \cdot & \cdot & \cdot & \cdot & \cdot & \cdot & & \sigma_{\varphi_n\omega_n} & \sigma_{\omega_n}^2 & \sigma_{\omega_n\kappa_n} & \cdot & \cdot & \cdot \\
\cdot & \cdot & 0 & \cdot & \cdot & \cdot & \cdot & \cdot & 0 & \cdot & \cdot & \cdot & \cdots & \sigma_{\varphi_n\kappa_n} & \sigma_{\omega_n\kappa_n} & \sigma_{\kappa_n}^2 & \cdot & \cdot & \cdot \\
\cdot & \cdot & \cdot & \sigma_{r_1r_n} & \cdot & \cdot & \cdot & \cdot & \cdot & \sigma_{r_2r_n} & \cdot & \cdot & & \cdot & \cdot & \cdot & \sigma_{r_n}^2 & \cdot & \cdot \\
\cdot & \cdot & \cdot & \cdot & \sigma_{p_1p_n} & 0 & \cdot & \cdot & \cdot & \cdot & \sigma_{p_2p_n} & 0 & & \cdot & \cdot & \cdot & \cdot & \sigma_{p_n}^2 & \cdot \\
0 & \cdot & \cdot & \cdot & 0 & \sigma_{y_1y_n} & 0 & \cdot & \cdot & \cdot & 0 & \sigma_{y_2y_n} & & 0 & \cdot & \cdot & \cdot & \cdot & \sigma_{y_n}^2
\end{array}\right] \quad (11)$$

This relation shows how the temporal correlation between the IMU/GPS attitude populates the variance-covariance matrix. The question how to find the actual correlation values will be addressed in the following section. For the moment, we assume that these are known and we care only about finding the proper weights for our least-square estimate of the boresight. When applying Equations (4) and (5), the weight matrix $P = (Q_{ll})^{-1}$ with Q_{ll} as given in (11). The estimated accuracy of the boresight vector x will then be

$$\hat{\sigma}_{\hat{x}} = \hat{\sigma}_0 \sqrt{N_{\hat{x}}^{-1}}$$
$$\hat{\sigma}_0 = \sqrt{\hat{v}^t P \hat{v} / (n-1)} \quad , \qquad \hat{v} = l - A\hat{x} \quad (12)$$

When estimating the boresight angles individually, the corresponding cofactors matrices Q_{lla}, Q_{llb}, Q_{llc} need to be extracted from the 'global' Q_{xx} as presented in the Appendix. The weighted average estimate can also be calculated by (5) when replacing A, P and l with

$$A^t = \begin{bmatrix} 1 & 1 & \cdots & 1 \end{bmatrix}_n, \quad l^t = \begin{bmatrix} e_{a_1} & e_{a_2} & \cdots & e_{a_n} \end{bmatrix}, \quad P = Q_{ll_a}^{-1}, \quad \text{(the same for } b, c). \quad (13)$$

4. Temporal Correlations in IMU/GPS Attitude

In previous section we described the necessary modifications of the '2-steps' boresight estimate to account for correlations in the IMU/GPS attitude. We have seen that such modification is relatively simple, as it only involves particular population of the Q_{ll} matrix (11). So far, nothing was said about the actual values of these cofactors. To address this topic we shall look first on some basic elements surrounding strapdown inertial sensors and navigation that is widely covered in the literature [10], [11].

[2] The user has usually an access only to RMS values of roll, pitch and yaw and not to the full KF variance and covariance matrix.

Systematic and random types of errors are present in all types of inertial instruments. Their magnitude and shape vary with the physical principals of the sensors, quality and make. However, in all cases the inertial navigation will bear a time dependent error structure. We are certainly interested to know to which extend the time correlation is controlled by the external measurements, i.e. integration with carrier phase DGPS data. This will mainly depend on the three aspects:

- IMU error behavior (usually well described by its manufacturer)
- KF setup that models this behavior (i.e. filter states and its parameters, processing noise, etc.)
- Trajectory profile and type of aiding (i.e. acceleration profile, updates: position, velocity, azimuth, etc.)

There is no doubt that the level of dependencies is relatively complex and generally varies from case to case. Therefore, we will try to present only the essentials using an example of a particular sensor and particular flying pattern over a small calibration field used for boresight determination. We shall consider two units of similar accuracy that are frequently used in direct georeferencing; Litton LN200-A1 or Honeywell HG 1700. The manufacture characteristics of the former are summarized in Table 2.

Performance Gyro		Performance Accelerometer	
Bias Repeatability	1^{O}/hr	Bias Repeatability	200 μg
Bias Variation	0.35^{O} /hr 1σ with T=100s	Bias Variation	50 μg 1σ with T=60s
Scale Factor Stability	100 ppm 1σ	Scale Factor Stability	300 ppm 1σ
Random Walk	0.04^{O}/√hr PSD level	White Noise	50 μg /√Hz PSD level

Table 2. Extract from LN-200 A1 IMU characteristics.

The sensor behaviour is reflected in the KF of an inertial navigator. The filter thus includes apart from the navigation states additional ones that model constant and short-term drifts as well as scale factors, etc. An attempt is then made to estimate these error states by means of external measurements. Here the trajectory profile and type of updates play an important role as they influence the resulting accuracy and the remaining level of correlation among the states (error coupling). The information about the time correlation and remaining dependencies is contained in the filter dynamic and variance-covariance matrices, respectively. Boresight determination via the ‘reversed 1-step’ method (Table 1) would account for such coupling quite naturally. As for the other approaches, a special output from the KF ought to be made, which is rarely the case. To circumvent the need of software upgrade for the end-users, we suggest the following approximation.

Considering the usual case of single-antenna GPS aiding, the gyro biases and scale-factors first propagate to the attitude state that will finally influence also the velocity and position states. The link from the attitude error to the velocity error is coupled with the magnitude of the specific force and thus also with accelerometer errors. In roll and pitch channels, this coupling is relatively strong due to presence of the gravity component, while in the azimuth channels this depends entirely on the extend of the vehicle manoeuvres [1]. It means that the azimuth error state becomes well estimated only during significant horizontal acceleration that is usually related to the large heading manoeuvres as shown in Figure 1. At this stage the attitude uncertainty decreases and also decorrelates from other states. Considering the bias variation of the LN-200 (correlation time 60-100s), the previously well-estimated error states decorrelate from its previously estimated value fairly quickly once flying into the straight line regardless of the position or velocity updates. Having said this and considering the fact that the boresight calibration is usually executed in few flight lines of short duration [12], the temporal correlation of the KF resembles that of the physical model (Table 2). In other words, the attitude time dependencies correspond well to the short-term gyro correlations. These are usually modelled within the KF by Gauss-Markov process; however, our empirical experience favours Gaussian function type:

$$\rho(t, t+\Delta t) = e^{\frac{-\Delta t^2}{T^2}} \tag{14}$$

Where, Δt is the time between 2 images within the same flight line and T is the bias variation correlation time. Knowing the accuracy of attitude (output of the navigation software) the temporal covariances in (11) can be computed as

$$\sigma_{y_t, y_{t+\Delta t}} = \rho_{t,t+\Delta t}\sigma_{y_t}\sigma_{y_{t+\Delta t}} \text{ , the same for } r,p. \tag{15}$$

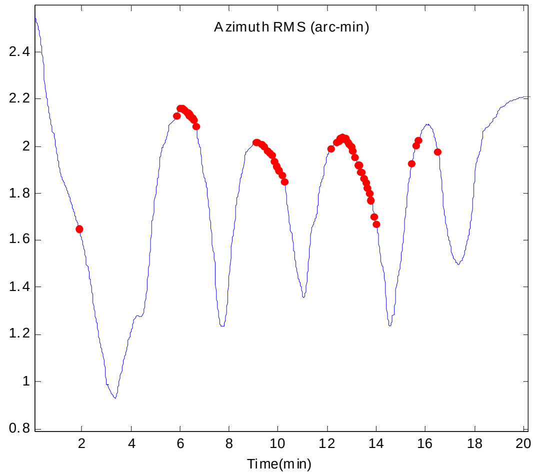

Figure 1: IMU/GPS heading accuracy with image events.

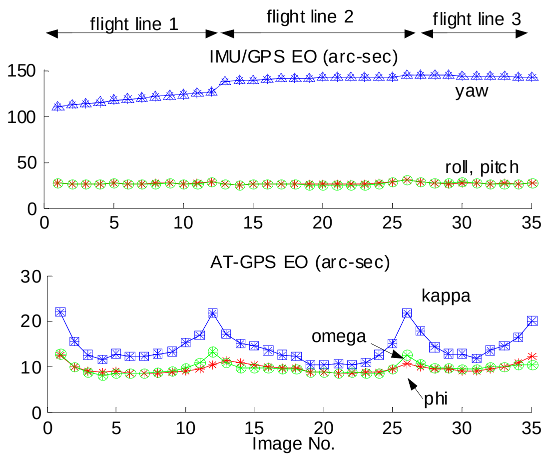

Figure 2: Attitude accuracy of IMU/GPS and AT for each image.

5. Numerical Examples

Here we examine practical influences of the presented approach on boresight determination. A second generation of a fully digital system originally developed for precise mapping of natural hazard areas[13] will serve the purpose.[3] The system integrates a Hasselblad Biogon/Kodak Proback Plus 16Mpix digital camera with 400 Hz outputs of the LN-200 A1 IMU and Legacy GD GPS receivers. The system small size and low weight (7kg) permits a hand-held use practically on any helicopter with minimum installation time.

We will consider two flights, both at a scale of about 1:10 000. The first for boresight calibration, the second for its application in direct georeferencing. The test zone consists of approximately 3x7 image block and 24 check-points ($\sigma \cong 3cm$). The tight points were measured manually and the AT-GPS aided solution was used as an input to the '2-steps' procedure (with and without time correlation). In parallel '1-step' boresight determination was calculated using [6]. The obtained boresight angles were then tested in the second flight that applied only forward intersection. Table 3 compares the boresight mean and accuracy estimate with the georeferencing residuals obtained in the check flight.

Method	**Calibration** Flight 1:10000 Boresight Estimation						**Application** Flight 1:10000 RMS Forward Intersections 24 checkpoints		
	Estimated **MEAN** (deg)			Estimated **ACCURACY** (deg)			Image Space (µm)	Object Space (m)	
	roll	pitch	yaw	roll	pitch	yaw		X, Y	Z
1-step (BINGO-F)	-0.003	-0.311	0.242	0.003	0.003	0.003	10	•	•
2-steps **Without** time correlation	-0.003	-0.310	0.240	0.002	0.001	0.002	9	0.15	0.17
2-steps Using time correlation	-0.004	-0.309	0.235	0.006	0.003	**0.010**	**7**	0.10	0.14

Table 3: Comparisons between different approaches to boresight determination with respect to resulting mapping accuracy.

As can be seen from this table, the 1-step and 2-steps estimates have similar mean values when no temporal correlations are considered. Both approaches are also too confident in the resulting accuracy, although not as extreme as reported in [8]. The size of residuals in direct georeferencing is also comparable. Once the attitude temporal correlations are considered the Q_{ll} matrix becomes populated outside the main diagonal as shown in Figure 3. As a result, the almost uniform IMU/GPS attitude accuracies for the image events (Figure 2) will not

[3] Intended comparison within the framework of OEEPE testing [4] was unfortunately not possible, as the needed information about the IMU/GPS data and the trajectory accuracy has not been made available.

longer appear flat in the cofactors, where the less correlated estimates receive higher weights (Figure 4). As explained in the previous section, the impact of this process is naturally most pronounced in the azimuth where a substantial change of the mean value is observed. This correlation process also raises the estimates uncertainty that becomes more realistic for the given type of IMU. Although having lower accuracy, the resulting mean is most likely less biased, which demonstrates itself by the increase of the mapping accuracy that reaches sub-pixel level (Table 3).

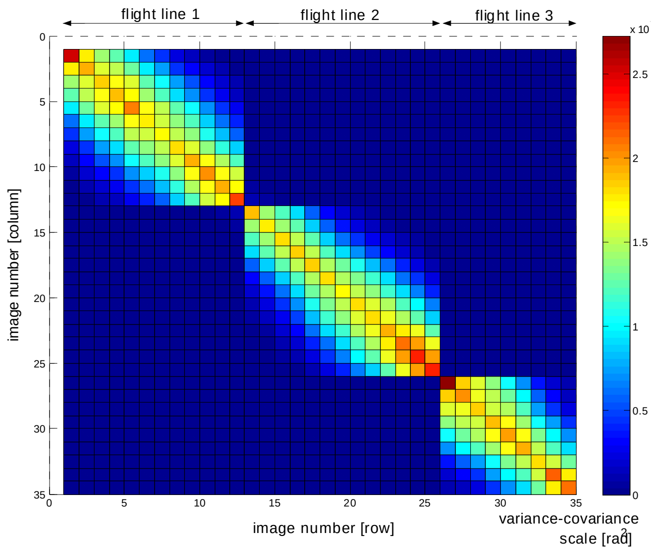

Figure 3: Q_{ll} matrix with IMU/GPS temporal correlations.

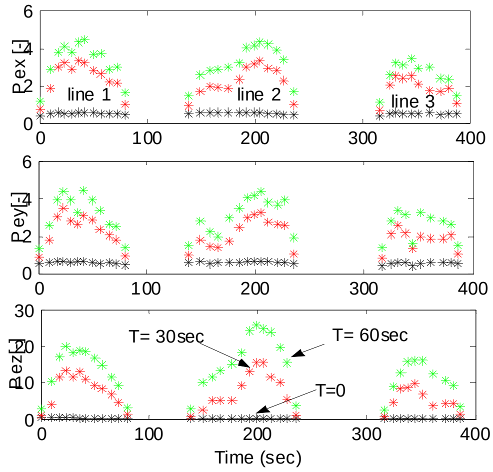

Figure 4: Impact of temporal correlation on the adjustment cofactors (weights) for IMU/GPS attitude.

6. Concluding Notes

This contribution aimed to highlight the significance of temporal correlation in the IMU/GPS data with respect to the boresight determination. Our investigations were motivated by the following reasons:

- The inertial navigator KF/smoother provides an optimum trajectory estimate that is subject to the external measurements and the trajectory dynamic encountered.
- The observability of some of the KF/smoother states is limited when needed the most (i.e. during the flight lines). Considering this fact together with an instrument error model, assuming 'randomness' in the attitude estimate few seconds apart (a usual interval between successive photographs) is certainly not correct.
- Currently proposed methods of boresight determination seem to be ignoring this fact, the result of which can lead to optimistic accuracies and biased mean values.

In Sections 2 and 3 we adapted the conventional '2-steps' boresight estimate method to reflect the time correlation in IMU/GPS data by introducing particular population of the global Q_{ll} matrix. Similar adaptation could be also envisaged in the AT software. However, with the '2-steps' method the user could keep certain independence of the needed revisions. The correct population of the Q_{ll} remains a subject of research, although the following can already be concluded:

- The information about the temporal correlations in the IMU/GPS orientation is relatively complex and the best information source is the Kalman Filter of an inertial navigator.
- When the above information is not available to the user, considering the physical model for a given IMU can make a good approximation given the small image block used for boresight calibration.

Finally, empirical testing has been made that supported the theoretical expectations:

- Considering the temporal correlation leads to important changes in the boresight mean value.
- The resulting accuracy estimate of boresight angles is more realistic.
- Application of such estimated boresight increases the mapping accuracy.

Acknowledgement

Julien Vallet and Jean-François Rolle are acknowledged in providing their expertise in photogrammetry, image measurement and flight execution. Babi Dana is thanked for revising the manuscript.

Bibliography

1. Skaloud, J., *Optimizing Georeferencing of Airborne Survey Systems by INS/DGPS*, in *Geomatics Engineering*. 1999, University of Calgary: Alberta, Canada.
2. Bäumker, M. and F.J. Heimes. *New Calibration and Computing Method for Direct Georeferencing of Image and Scanner Data Using the Position and Angular Data of an Hybrid Inertial Navigation System*. in *Integrated Sensor Orientation, Proc. of the OEEPE Workshop*. 2001. Hanover: CD-ROM.
3. Mostafa, M. *Camera/IMU Boresight Calibration: New Advances and Performance Analysis*. in *ASPRS Annual Meeting*. 2002. Washington, DC, USA.
4. Heipke, C., K. Jacobsen, and H. Wegmann, *Integrated Sensor Orientation*. OEEPE Official Publication. Vol. 43. 2002, Frankfurt am Main: Verlag Bundesamt für Kartographie und Geoäsie.
5. Pinto, L. and G. Forlani. *A Single Step Calibration Procedure for IMU/GPS In Aerial Photogrammetry*. in *Photogrammetric Computer Vision, ISPRS Commission III Symposium*. 2002. Graz, Austria.
6. Kruck, E. *Combined IMU and sensor calibration with BINGO-F*. in *Integrated Sensor Orientation, Proc. of the OEEPE Workshop "*. 2001. Hannover: CD-ROM.
7. Cramer, M. and D. Stallmann. *System Calibration For Direct Georeferencing*. in *Photogrammetric Computer Vision, ISPRS Commission III Symposium*. 2002. Graz, Austria.
8. Wegmann, H. *Image Orientation by Combined (A)AT with GPS and IMU*. in *ISPRS Comission I Mid-Term Symposium in conjunction with Pecora 15/Land Satellite Information IV Conference*. 2002. Denver, Co, USA.
9. Mostafa, M. *Quality Control of Direct Georeferencing Data*. in *ISPRS Comission I Mid-Term Symposium in conjunction with Pecora 15/Land Satellite Information IV Conference*. 2002. Denver, CO USA.
10. Titterton, D.H. and J.L. Weston, *Strapdown inertial navigation technology*. Part of IEE radar, sonar, navigation and avionics series. 1997: Stevenage, U.K. 455.
11. Grewal, M.S., L.R. Weill, and A.P. Andrews, *Global Positioning Systems, Inertial Navigation, and Integration*. 2001: John Wiley & Sons, Inc. 392.
12. Colomina, I., *GPS, INS And Aerial Triangulation: What Is The Best Way for The Operational Determination of Photogrammetric Image Orientation*, in *Proc. ISPRS Comm. III*. 1999: Munchen. p. 212-130.
13. Skaloud, J. and J. Vallet. *High Accuracy Handheld Mapping System for Fast Helicopter Deployment*. in *Joint International Symposium on Geospatial Theory, Processing and Applications, ISPRS Comm. IV*. 2002. Ottawa, Canada.

Appendix - Q_{xx}

In general case, the structure of Q_{xx} resulting from (8) is relatively complicated. Nevertheless, considering the special case of small rotation (i.e. approximation by skew-symmetric matrix is valid), following simplifications can be made:

- The elements on the diagonal (b_{11}, b_{22}, b_{33}) are constants, therefore their variance-covariance is 0.
- The parameters a(b_{23}, b_{32}), b (b_{13}, b_{31}) and c (b_{12}, b_{21}) and their corresponding variance-covariance values occur twice for one image

Hence,

Q_{xx} [$9n$ x $9n$] ≈

$$
\begin{array}{c}
\begin{array}{ccccccccccccccccccc}
b_{11}^{1} & b_{12}^{1} & b_{13}^{1} & b_{21}^{1} & b_{22}^{1} & b_{23}^{1} & b_{31}^{1} & b_{32}^{1} & b_{33}^{1} & & b_{11}^{n} & b_{12}^{n} & b_{13}^{n} & b_{21}^{n} & b_{22}^{n} & b_{23}^{n} & b_{31}^{n} & b_{32}^{n} & b_{33}^{n}
\end{array}
\\
\approx
\left[\begin{array}{ccccccccccccccccccc}
0 & 0 & 0 & 0 & 0 & 0 & 0 & 0 & 0 & \cdots & & & & & & & & & \\
0 & \sigma_{c_1}^{2} & \sigma_{c_1 b_1} & -1 & 0 & \sigma_{a_1 c_1} & \sigma_{c_1 b_1} & \sigma_{a_1 c_1} & 0 & \cdots & & & & & & & & & \\
0 & \sigma_{c_1 b_1} & \sigma_{b_1}^{2} & \sigma_{c_1 b_1} & 0 & \sigma_{a_1 b_1} & -1 & \sigma_{a_1 b_1} & 0 & \cdots & & & & & & & & & \\
0 & -1 & \sigma_{c_1 b_1} & \sigma_{c_1}^{2} & 0 & \sigma_{a_1 c_1} & \sigma_{c_1 b_1} & \sigma_{a_1 c_1} & 0 & \cdots & & & & & & & & & \\
0 & 0 & 0 & 0 & 0 & 0 & 0 & 0 & 0 & \cdots & & & & & & & & & \\
0 & \sigma_{a_1 c_1} & \sigma_{a_1 b_1} & \sigma_{a_1 c_1} & 0 & \boxed{\sigma_{a_1}^{2}} & \sigma_{a_1 b_1} & -1 & 0 & \cdots & & & & & & \boxed{\sigma_{a_1 a n_1}} & & & \\
0 & \sigma_{c_1 b_1} & -1 & \sigma_{c_1 b_1} & 0 & \sigma_{a_1 b_1} & \sigma_{b_1}^{2} & \sigma_{a_1 b_1} & 0 & \cdots & & & & & & & & & \\
0 & \sigma_{a_1 c_1} & \sigma_{a_1 b_1} & \sigma_{a_1 c_1} & 0 & -1 & \sigma_{a_1 b_1} & \sigma_{a_1}^{2} & 0 & \cdots & & & & & & & & & \\
0 & 0 & 0 & 0 & 0 & 0 & 0 & 0 & 0 & \cdots & & & & & & & & & \\
\vdots & \vdots & \vdots & \vdots & \vdots & \vdots & \vdots & \vdots & \vdots & \ddots & \vdots & \vdots & \vdots & \vdots & \vdots & \vdots & \vdots & \vdots & \vdots \\
 & & & & & & & & & \cdots & 0 & 0 & 0 & 0 & 0 & 0 & 0 & 0 & 0 \\
 & & & & & & & & & \cdots & 0 & \sigma_{c_n}^{2} & \sigma_{c_n b_n} & -1 & 0 & \sigma_{a_n c_n} & \sigma_{c_n b_n} & \sigma_{a_n c_n} & 0 \\
 & & & & & & & & & \cdots & 0 & \sigma_{c_n b_n} & \sigma_{b_n}^{2} & \sigma_{c_n b_n} & 0 & \sigma_{a_n b_n} & -1 & \sigma_{a_n b_n} & 0 \\
 & & & & & & & & & \cdots & 0 & -1 & \sigma_{c_n b_n} & \sigma_{c_n}^{2} & 0 & \sigma_{a_n c_n} & \sigma_{c_n b_n} & \sigma_{a_n c_n} & 0 \\
 & & & & & & & & & \cdots & 0 & 0 & 0 & 0 & 0 & 0 & 0 & 0 & 0 \\
 & & & & & \boxed{\sigma_{a_1 a n_1}} & & & & \cdots & 0 & \sigma_{a_n c_n} & \sigma_{a_n b_n} & \sigma_{a_n c_n} & 0 & \boxed{\sigma_{a_n}^{2}} & \sigma_{a_n b_n} & -1 & 0 \\
 & & & & & & & & & \cdots & 0 & \sigma_{c_n b_n} & -1 & \sigma_{c_n b_n} & 0 & \sigma_{a_n b_n} & \sigma_{b_n}^{2} & \sigma_{a_n b_n} & 0 \\
 & & & & & & & & & \cdots & 0 & \sigma_{a_n c_n} & \sigma_{a_n b_n} & \sigma_{a_n c_n} & 0 & -1 & \sigma_{a_n b_n} & \sigma_{a_n}^{2} & 0 \\
 & & & & & & & & & \cdots & 0 & 0 & 0 & 0 & 0 & 0 & 0 & 0 & 0
\end{array}\right]
\end{array}
\tag{16}
$$

As only the variance-covariance factors for the three parameters (a, b, c) of the skew-symmetric matrix are used to compute the weighted solution, the Q_{xx} can be split into 3 separate matrices (Q_{lla}, Q_{llb}, Q_{llc},) needed in (13). This is achieved by extracting the corresponding lines and columns as indicated by the boxes in (14):

$$
Q_{ll\,a} = \begin{bmatrix}
\sigma_{a_1}^{2} & \sigma_{a_1 a_2} & . & . & \sigma_{a_1 a_n} \\
\sigma_{a_1 a_2} & \sigma_{a_2}^{2} & . & . & . \\
. & . & . & . & . \\
. & . & . & \sigma_{a_{n-1}}^{2} & \sigma_{a_{n-1} a_n} \\
\sigma_{a_n a^1} & . & . & \sigma_{a_{n-1}} \sigma_{a_n} & \sigma_{a_n}^{2}
\end{bmatrix}
\tag{17}
$$

The same procedure applies to Q_{llb} and Q_{llc}.